

# The meson-exchange model for the $\Lambda\bar{\Lambda}$ interaction

Lu Zhao<sup>1,2\*</sup>, Ning Li<sup>3</sup>, Shi-Lin Zhu<sup>3</sup>, Bing-Song Zou<sup>1,4†</sup>

1. Institute of High Energy Physics and Theoretical Physics Center for Science Facilities, CAS, Beijing 100049, China

2. University of Chinese Academy of Sciences, Beijing 100049, China

3. Department of Physics and State Key Laboratory of Nuclear Physics and Technology, Peking University, Beijing 100871, China

4. State Key Laboratory of Theoretical Physics, Institute of Theoretical Physics, CAS, Beijing 100190, China

In the present work, we apply the one-boson-exchange potential (OBEP) model to investigate the possibility of  $Y(2175)$  and  $\eta(2225)$  as bound states of  $\Lambda\bar{\Lambda}(^3S_1)$  and  $\Lambda\bar{\Lambda}(^1S_0)$  respectively. We consider the effective potential from the pseudoscalar  $\eta$ -exchange and  $\eta'$ -exchange, the scalar  $\sigma$ -exchange, and the vector  $\omega$ -exchange and  $\phi$ -exchange. The  $\eta$  and  $\eta'$  meson exchange potential is repulsive force for the state  $^1S_0$  and attractive for  $^3S_1$ . The results depend very sensitively on the cutoff parameter of the  $\omega$ -exchange ( $\Lambda_\omega$ ) and least sensitively on that of the  $\phi$ -exchange ( $\Lambda_\phi$ ). Our result suggests the possible interpretation of  $Y(2175)$  and  $\eta(2225)$  as the bound states of  $\Lambda\bar{\Lambda}(^3S_1)$  and  $\Lambda\bar{\Lambda}(^1S_0)$  respectively.

PACS numbers: 13.75.-n, 13.75.Cs, 14.20.Gk

## I. INTRODUCTION

In 2005, the BABAR Collaboration announced the first observation of  $Y(2175)$  in the initial-state-radiation process  $e^+e^- \rightarrow \gamma_{ISR}\phi(1020)f_0(980)$ , and the experimental data indicated that it is a  $J^{PC} = 1^{--}$  resonance with mass  $m = 2175 \pm 10 \pm 15$  MeV and width  $\Gamma = 58 \pm 16 \pm 20$  MeV [1]. Later, the BES Collaboration also observed the similar structure in the decay of  $J/\psi \rightarrow \eta\phi f_0(980)$  with about  $5\sigma$  significance [2]. Since both  $Y(2175)$  and  $Y(4260)$  are produced in  $e^+e^-$  annihilation and exhibit similar decay patterns,  $Y(2175)$  might be interpreted as an  $s\bar{s}$  analogue of the  $Y(4260)$ , or as an  $s\bar{s}s\bar{s}$  state that decays predominantly to  $\phi(1020)f_0(980)$  [1]. So far, the interpretations of  $Y(2175)$  include  $q\bar{q}g$  hybrid [3, 4], tetraquark state [5–7], excited  $1^{--}$   $s\bar{s}$  state [8] and resonance state of  $\phi K\bar{K}$  [9, 10]. Besides, there are also some other very interesting speculations on  $Y(2175)$  [11–13].

The  $\eta(2225)$  was first observed by the MARK-III collaboration in the radiative decays  $J/\psi \rightarrow \gamma\phi\phi$  [14]. Its mass and width were measured to be 2220 MeV and 150 MeV respectively while its quantum numbers was assigned to be  $J^{PC} = 0^{-+}$ . Later, the BES Collaboration also observed a signal around 2240 MeV from a high statistics study of  $J/\psi \rightarrow \gamma\phi\phi$  in the  $\gamma K^+ K^- K_L^0 K_L^0$  final state [13]. In Ref. [15], the authors investigated the strong decays of  $^3S_0$  and  $4^1S_0$  within the the framework of the  $^3P_0$  meson decay model and found that the  $\eta(2225)$  was very hard to interpreted as the  $3^1S_0$   $s\bar{s}$  state but a good candidate for  $4^1S_0$   $s\bar{s}$  state.

Note that both  $Y(2175)$  and  $\eta(2225)$  are close to the threshold of  $\Lambda\bar{\Lambda}$ . If these two states are not the conventional  $s\bar{s}$  excited state in the quark model, an interesting interpretation is that they might be the loosely bound states of  $\Lambda\bar{\Lambda}$ . If we only consider the S-wave molecular states,  $Y(2175)$  and  $\eta(2225)$  should be assigned as  $\Lambda\bar{\Lambda}(^3S_1)$  and  $\Lambda\bar{\Lambda}(^1S_0)$  respectively. Actually, more than thirty year ago, Dover, *et al.* studied the bound states of  $\Lambda\bar{\Lambda}$  with the orbital angular quantum  $L \geq 1$

within the meson-exchange model. The interested readers can refer to Ref. [16].

In the present work, we apply the one-boson-exchange potential (OBEP) model, which works very well in interpreting the deuteron, to investigate the possibility of  $Y(2175)$  and  $\eta(2225)$  as bound states of  $\Lambda\bar{\Lambda}(^3S_1)$  and  $\Lambda\bar{\Lambda}(^1S_0)$  respectively. As an effective theory, the one-boson-exchange potential model contains the long-range force coming from the pion-exchange, the medium-range force coming from the sigma-exchange and the short-range force coming from the heavier vector rho/omega/phi-exchange. So far, lots of efforts have been spent on the investigation of the possible bound states composed of a pair of mesons or baryons within the one-boson-exchange potential framework. In Ref. [17], the authors performed a systematic study of the possible bound states composed of a pair of heavy meson and heavy anti-meson within the one-boson-exchange framework. In Ref. [18], using the Bonn meson-exchange model, the authors performed a detailed and systematic study of the nucleon-nucleon interaction. The one-boson-exchange potential model leads to an excellent description of the deuteron data,  $NN$  scattering phase shifts and many other observables.

The paper is organized as follows. After the introduction, we present the scattering amplitude in Section II and the effective potential in Section III. The numerical results are given in Section IV. We discuss our results in Section V.

## II. SCATTERING AMPLITUDE

In the present work, we apply the Bonn meson-exchange model, which works very well in the description of the deuteron, to calculate the effective interaction potential of  $\Lambda\bar{\Lambda}$ . In this one-boson-exchange potential (OBEP) model, the long-range  $\pi$ -exchange, the medium-range  $\eta$ -exchange and  $\sigma$ -exchange, and the short-range  $\omega$ -exchange and  $\rho$ -exchange combine to account for the interaction of the loosely bound deuteron [18]. Given that the system of  $\Lambda\bar{\Lambda}$  is an isoscalar, the exchanged mesons include  $\eta$ ,  $\eta'$ ,  $\sigma$ ,  $\omega$ . Besides, the heavier  $\phi$  should also account for the interaction of  $\Lambda\bar{\Lambda}$ . The Feynman

\*Email: zhaolu@ihep.ac.cn

†Email: zoubs@itp.ac.cn

diagram at the tree level is shown in Fig. 1.

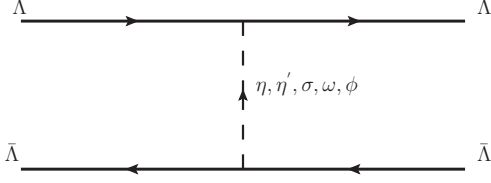


FIG. 1: The Feynman diagram at the tree level.

In our study, we first derive the baryon-baryon potential  $V_{\Lambda\Lambda}(r)$ . Starting from  $V_{\Lambda\Lambda}$ , we directly obtain  $V_{\Lambda\bar{\Lambda}}$  by reversing the terms corresponding to the exchange of a meson of odd G-parity,  $G^i$ , i.e.,

$$V_{\Lambda\bar{\Lambda}}(r) = \sum_i (-1)^{G_i} V_{\Lambda\Lambda}^i(r). \quad (1)$$

The effective Lagrangian densities describing the  $\eta\Lambda\Lambda$ ,  $\eta'\Lambda\Lambda$ ,  $\sigma\Lambda\Lambda$  and  $\omega\Lambda\Lambda$ ,  $\phi\Lambda\Lambda$  vertices are

$$\mathcal{L}_{\eta\Lambda\Lambda} = -ig_{\eta\Lambda\Lambda} \bar{\Psi} \gamma_5 \Psi \eta, \quad (2)$$

$$\mathcal{L}_{\eta'\Lambda\Lambda} = -ig_{\eta'\Lambda\Lambda} \bar{\Psi} \gamma_5 \Psi \eta', \quad (3)$$

$$\mathcal{L}_{\sigma\Lambda\Lambda} = g_{\sigma\Lambda\Lambda} \bar{\Psi} \sigma \Psi, \quad (4)$$

$$\mathcal{L}_{\omega\Lambda\Lambda} = -g_{\omega\Lambda\Lambda} \bar{\Psi} \gamma_\mu \omega^\mu \Psi + \frac{f_{\omega\Lambda\Lambda}}{2m_\Lambda} \bar{\Psi} \sigma_{\mu\nu} \Psi \partial^\mu \omega^\nu, \quad (5)$$

and

$$\mathcal{L}_{\phi\Lambda\Lambda} = -g_{\phi\Lambda\Lambda} \bar{\Psi} \gamma_\mu \phi^\mu \Psi + \frac{f_{\phi\Lambda\Lambda}}{2m_\Lambda} \bar{\Psi} \sigma_{\mu\nu} \Psi \partial^\mu \phi^\nu. \quad (6)$$

In the above,  $\Psi$  is the Dirac-spinor for the spin- $\frac{1}{2}$  particle of  $\Lambda$ . Actually, there only exists the vector form for the  $NN$  system with the  $\omega$ -exchange,  $f_{\omega NN}/g_{\omega NN} = 0$  [18]. Thus with the  $SU(3)$  - flavor symmetry,  $f_{\omega\Lambda\Lambda} = f_{\phi\Lambda\Lambda} = 0$ . Therefore, the Eqs (5) and (6) change into

$$\mathcal{L}_{\omega\Lambda\Lambda} = -g_{\omega\Lambda\Lambda} \bar{\Psi} \gamma_\mu \omega^\mu \Psi, \quad (7)$$

and

$$\mathcal{L}_{\phi\Lambda\Lambda} = -g_{\phi\Lambda\Lambda} \bar{\Psi} \gamma_\mu \phi^\mu \Psi. \quad (8)$$

With the Lagrangians given in Eqs (2-8), we can derive the scattering amplitude of Fig. 1. In our calculation we adopt the Dirac spinor as

$$u(\vec{q}, s) = \sqrt{\frac{E+M}{2M}} \begin{pmatrix} \chi_s \\ \frac{\vec{\sigma} \cdot \vec{q}}{E+M} \chi_s \end{pmatrix} \quad (9)$$

and

$$\bar{u}(\vec{q}, s) \equiv u^\dagger(\vec{q}, s) \gamma^0 = \sqrt{\frac{E+M}{2M}} \left( \chi_s^\dagger \quad -\chi_s^\dagger \frac{\vec{\sigma} \cdot \vec{q}}{E+M} \right) \quad (10)$$

In the center-of-mass frame, the initial four-momentums are  $P_1(E_1, \vec{p})$  and  $P_2(E_2, -\vec{p})$  while the final four-momentums are  $P_3(E_1, \vec{p}')$  and  $P_4(E_2, -\vec{p}')$ , see Fig.2. Thus the four-momentum of propagator is

$$q = P_3 - P_1 = P_2 - P_4 = (0, \vec{p}' - \vec{p}) = (0, \vec{q}) \quad (11)$$

For the convenience of algebraic calculations, we make the following momentum substitution,

$$\vec{q} = \vec{p}' - \vec{p} \quad (12)$$

and

$$\vec{k} = \frac{1}{2}(\vec{p}' + \vec{p}). \quad (13)$$

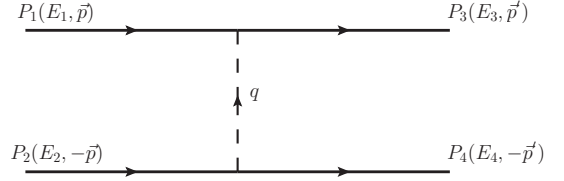


FIG. 2: The four momentum for the  $\Lambda\bar{\Lambda}$  system.

In our calculation, we make the nonrealistic approximation and keep the terms up to order of  $\frac{1}{m_\Lambda^2}$ . The scattering amplitudes are

$$\begin{aligned} iM_\eta &= g_{\eta\Lambda\Lambda}^2 \bar{u}_\Lambda \gamma_5 u_\Lambda \frac{i}{q^2 - m_\eta^2} \bar{u}_\Lambda \gamma_5 u_\Lambda \\ &= i \frac{g_{\eta\Lambda\Lambda}^2}{\vec{q}^2 + m_\eta^2} \frac{(\vec{\sigma}_1 \cdot \vec{q})(\vec{\sigma}_2 \cdot \vec{q})}{4m_\Lambda^2}, \end{aligned} \quad (14)$$

$$\begin{aligned} iM_\sigma &= -g_{\sigma\Lambda\Lambda}^2 \bar{u}_\Lambda u_\Lambda \frac{i}{q^2 - m_\sigma^2} \bar{u}_\Lambda u_\Lambda \\ &= i \frac{g_{\sigma\Lambda\Lambda}^2}{\vec{q}^2 + m_\sigma^2} \left[ 1 - \frac{\vec{k}^2}{2m_\Lambda^2} + \frac{\vec{q}^2}{8m_\Lambda^2} + i \frac{\vec{S} \cdot (\vec{k} \times \vec{q})}{2m_\Lambda^2} \right], \end{aligned} \quad (15)$$

and

$$\begin{aligned} iM_\omega &= -g_{\omega\Lambda\Lambda}^2 \bar{u}_\Lambda \gamma^\mu u_\Lambda i \frac{-g_{\mu\nu} + \frac{q_\mu q_\nu}{m_\omega^2}}{q^2 - m_\omega^2} \bar{u}_\Lambda \gamma^\nu u_\Lambda \\ &= i \frac{g_{\omega\Lambda\Lambda}^2}{\vec{q}^2 + m_\omega^2} \left[ 1 - \frac{\vec{q}^2}{8m_\Lambda^2} + \frac{3\vec{k}^2}{2m_\Lambda^2} + i \frac{3\vec{S} \cdot (\vec{k} \times \vec{q})}{2m_\Lambda^2} \right. \\ &\quad \left. - \frac{(\vec{\sigma}_1 \cdot \vec{\sigma}_2) \cdot \vec{q}^2}{4m_\Lambda^2} + \frac{(\vec{\sigma}_1 \cdot \vec{q})(\vec{\sigma}_2 \cdot \vec{q})}{4m_\Lambda^2} \right], \end{aligned} \quad (16)$$

TABLE I: The coupling constants  $g_{\alpha\Lambda\Lambda}$ , the masses of the exchanged mesons taken from PDG [19] and the cutoff parameters  $\Lambda_\alpha$ .

$\alpha$	$\eta$	$\eta'$	$\sigma$	$\omega$	$\phi$
$m_\alpha(\text{MeV})$	548.8	957.7	550.0	782.6	1019.5
$\frac{g_{\alpha\Lambda\Lambda}^2}{4\pi}$	4.473	9.831	3.459	8.889	2.222
$\Lambda_\alpha(\text{GeV})$	0.9	1.4	0.9	1.1	1.5

where  $\vec{S} = \frac{1}{2}(\vec{\sigma}_1 + \vec{\sigma}_2)$  is the total spin of  $\Lambda\bar{\Lambda}$ .  $iM_{\eta'}$  is similar to  $iM_\eta$  while  $iM_\phi$  is similar to  $iM_\omega$ . Making the substitutions  $g_{\eta\Lambda\Lambda} \rightarrow g_{\eta'\Lambda\Lambda}$  in Eq. (14) and  $g_{\omega\Lambda\Lambda} \rightarrow g_{\phi\Lambda\Lambda}$  in Eq. (16), one can straightforwardly obtain  $iM_{\eta'}$  and  $iM_\phi$  respectively.

The coupling constants for the nucleon-nucleon-meson have been fixed quite well by fitting the experimental data. In the present work, we take the values of  $g_{\alpha NN}$  from the Bonn meson-exchange model [18]. The values of the coupling constants  $g_{\alpha\Lambda\Lambda}$  can be derived from  $g_{\alpha NN}$  through the SU(3)-flavor symmetry. And they are

$$g_{\Lambda\Lambda\eta} = -\alpha \sqrt{\frac{4}{3}} g_{NN\pi} (\cos\theta + \sin\theta), \quad (17)$$

and

$$g_{\Lambda\Lambda\eta'} = \alpha \sqrt{\frac{4}{3}} g_{NN\pi} (\cos\theta - \sin\theta), \quad (18)$$

in which the quadratic Gell-Mann-Okubo mass formula is used and

$$\alpha \equiv D/(D+F) = 0.6, \quad (19)$$

$$g_{\Lambda\Lambda\sigma} = \frac{2}{3} g_{NN\sigma}, \quad (20)$$

$$g_{\Lambda\Lambda\omega} = \frac{2}{3} g_{NN\omega}, \quad (21)$$

$$g_{\Lambda\Lambda\phi} = \frac{1}{3} g_{NN\omega}. \quad (22)$$

The mass of  $\Lambda$  is taken as 1115.7 MeV from PDG [19]. We summarize the numerical values of the coupling constants and the masses of the exchanged mesons in Table I.

### III. INTERACTIONAL POTENTIAL

In the scattering theory of quantum mechanics, the relativistic S-matrix has the form

$$\langle f|S|i\rangle = \delta_{fi} + i\langle f|T|i\rangle = \delta_{fi} + (2\pi)^4 \delta^4(p_f - p_i) iM_{fi}, \quad (23)$$

in which the T-matrix is the interaction part of the S-matrix and  $M_{ij}$  is defined as the invariant matrix element when extracting the 4-momentum conservation of the T-matrix. The non-relativistic S-matrix has the form

$$\langle f|S|i\rangle = \delta_{fi} - 2\pi\delta(E_f - E_i) iV_{fi}. \quad (24)$$

After considering both the relativistic normalization and non-relativistic normalization, one gets the relationship between the interaction potential  $V_{fi}$  and the scattering amplitude  $M_{fi}$  in the momentum space.

$$V_{fi} = -\frac{M_{fi}}{\sqrt{\prod_f 2E_f} \sqrt{\prod_i 2E_i}} \approx -\frac{M_{fi}}{\sqrt{\prod_f 2m_f} \sqrt{\prod_i 2m_i}}. \quad (25)$$

Considering the structure effect of the baryons, we introduce one monopole form factor

$$F(q) = \frac{\Lambda^2 - m_{ex}^2}{\Lambda^2 - q^2} = \frac{\Lambda^2 - m_{ex}^2}{\Lambda^2 + \vec{q}^2}, \quad (26)$$

at each vertex. Here,  $\Lambda$  is the cutoff parameter and  $m_{ex}$  is the mass of the exchanged meson. To obtain the effective potentials of the  $\Lambda\bar{\Lambda}$  system, one needs to make the following Fourier Transformation,

$$V(\vec{k}, r) = \frac{1}{(2\pi)^3} \int d\vec{q}^3 e^{-i\vec{q}\cdot\vec{r}} V(\vec{q}, \vec{k}) F^2(\vec{q}), \quad (27)$$

and the following functions will be very helpful,

$$\begin{aligned} \mathcal{F}_1 &= \mathcal{F} \left\{ \frac{1}{\vec{q}^2 + m^2} \left( \frac{\Lambda^2 - m^2}{\Lambda^2 + \vec{q}^2} \right)^2 \right\} \\ &= mY(mr) - \Lambda Y(\Lambda r) - (\Lambda^2 - m^2) \frac{e^{-\Lambda r}}{2\Lambda}, \end{aligned} \quad (28)$$

$$\begin{aligned} \mathcal{F}_2 &= \mathcal{F} \left\{ \frac{\vec{q}^2}{\vec{q}^2 + m^2} \left( \frac{\Lambda^2 - m^2}{\Lambda^2 + \vec{q}^2} \right)^2 \right\} \\ &= -m^3 Y(mr) + m^2 \Lambda Y(\Lambda r) + (\Lambda^2 - m^2) \frac{\Lambda e^{-\Lambda r}}{2}, \end{aligned} \quad (29)$$

$$\begin{aligned} \mathcal{F}_3 &= \mathcal{F} \left\{ \frac{(\vec{\sigma}_1 \cdot \vec{q})(\vec{\sigma}_2 \cdot \vec{q})}{\vec{q}^2 + m^2} \left( \frac{\Lambda^2 - m^2}{\Lambda^2 + \vec{q}^2} \right)^2 \right\} \\ &= \frac{1}{3} \vec{\sigma}_1 \cdot \vec{\sigma}_2 \left[ m^2 \Lambda Y(\Lambda r) - m^3 Y(mr) + (\Lambda^2 - m^2) \Lambda \frac{e^{-\Lambda r}}{2} \right] \\ &\quad + \frac{1}{3} S_{12} \left[ -m^3 Z(mr) + \Lambda^3 Z(\Lambda r) \right. \\ &\quad \left. + (\Lambda^2 - m^2)(1 + \Lambda r) \frac{\Lambda}{2} Y(\Lambda r) \right] \\ &= (\vec{\sigma}_1 \cdot \vec{\sigma}_2) \mathcal{F}_{3a} + S_{12} \mathcal{F}_{3b}, \end{aligned} \quad (30)$$

$$\begin{aligned} \mathcal{F}_4 &= \mathcal{F} \left\{ \frac{\vec{k}^2}{\vec{q}^2 + m^2} \left( \frac{\Lambda^2 - m^2}{\Lambda^2 + \vec{q}^2} \right)^2 \right\} \\ &= \frac{m^3}{4} Y(Mr) - \frac{\Lambda^3}{4} Y(\Lambda r) - \frac{\Lambda^2 - m^2}{4} \left( \frac{\Lambda r}{2} - 1 \right) \frac{e^{-\Lambda r}}{r} \\ &\quad - \frac{1}{2} \left\{ \nabla^2, mY(mr) - \Lambda Y(\Lambda r) - \frac{\Lambda^2 - m^2}{2} \frac{e^{-\Lambda r}}{\Lambda} \right\} \\ &= \mathcal{F}_{4a} + \left\{ \nabla^2, \mathcal{F}_{4b} \right\}, \end{aligned} \quad (31)$$

$$= \mathcal{F}_{4a} + \left\{ \nabla^2, \mathcal{F}_{4b} \right\}, \quad (32)$$

and

$$\begin{aligned}\mathcal{F}_5 &= \mathcal{F} \left\{ i \frac{\vec{S} \cdot (\vec{q} \times \vec{k})}{\vec{q}^2 + m^2} \left( \frac{\Lambda^2 - m^2}{\Lambda^2 + \vec{q}^2} \right)^2 \right\} \\ &= \vec{S} \cdot \vec{L} \left[ -m^3 Z_1(mr) + \Lambda^3 Z_1(\Lambda r) + (\Lambda^2 - m^2) \frac{\Lambda e^{-\Lambda r}}{2r} \right] \\ &= \vec{S} \cdot \vec{L} \mathcal{F}_{5a}.\end{aligned}\quad (33)$$

In the above equations, the functions  $Y(x)$ ,  $Z(x)$  and  $Z_1(x)$  are defined as

$$Y(x) = \frac{e^{-x}}{x}, \quad (34)$$

$$Z(x) = \left( 1 + \frac{3}{x} + \frac{3}{x^2} \right) Y(x) \quad (35)$$

and

$$Z_1(x) = \left( \frac{1}{x} + \frac{1}{x^2} \right) Y(x). \quad (36)$$

With the help of Eqs. (28-33), one can easily write the effective potential of the system  $\Lambda\bar{\Lambda}$  as

$$V_\eta(r) = -\frac{g_{\Lambda\Lambda\eta}^2}{4\pi} \left( \frac{\vec{\sigma}_1 \cdot \vec{\sigma}_2}{4m_\Lambda^2} \mathcal{F}_{3a} + \frac{1}{4m_\Lambda^2} S_{12} \mathcal{F}_{3b} \right), \quad (37)$$

$$V_\sigma(r) = \frac{g_{\Lambda\Lambda\sigma}^2}{4\pi} \left( -\mathcal{F}_1 + \frac{1}{2m_\Lambda^2} \mathcal{F}_{4a} - \frac{1}{8m_\Lambda^2} \mathcal{F}_2 + \frac{1}{2m_\Lambda^2} \vec{S} \cdot \vec{L} \mathcal{F}_{5a} \right) \quad (38)$$

$$\begin{aligned}V_\omega(r) &= \frac{g_{\Lambda\Lambda\omega}^2}{4\pi} \left[ -\mathcal{F}_1 - \frac{3}{2m_\Lambda^2} \mathcal{F}_{4a} + \frac{1}{8m_\Lambda^2} \mathcal{F}_2 - \frac{3}{2m_\Lambda^2} \vec{S} \cdot \vec{L} \mathcal{F}_{5a} \right. \\ &\quad \left. + \frac{\vec{\sigma}_1 \cdot \vec{\sigma}_2}{4m_\Lambda^2} (\mathcal{F}_2 - \mathcal{F}_{3a}) - \frac{1}{4m_\Lambda^2} S_{12} \mathcal{F}_{3b} \right], \quad (39)\end{aligned}$$

The effective potentials for the  $\eta'$ -exchange and the  $\phi$ -exchange are similar to  $V_\eta$  and  $V_\omega$  respectively. One can directly obtain them by making substitutions  $g_{\eta\Lambda\Lambda} \rightarrow g_{\eta'\Lambda\Lambda}$  in Eq. 37 and  $g_{\omega\Lambda\Lambda} \rightarrow g_{\phi\Lambda\Lambda}$  in Eq. 39.

In order to make clear the specific roles of the exchanged mesons in the effective potentials of the  $\Lambda\bar{\Lambda}$  system, we adopt a set of values of the cutoff parameters based on the mass of the exchanged meson in Table I and plot the effective potential for states  $^1S_0$  and  $^3S_1$  in Fig. 3. From Fig 3 we can see that for the state  $^1S_0$  both the  $\eta$ -exchange and the  $\eta'$ -exchange provide repulsive force while the  $\phi$ -exchange, the  $\omega$ -exchange and the  $\sigma$ -exchange provide attractive force. For the state  $^3S_1$ , the  $\phi$ -exchange and the  $\omega$ -exchange provide repulsive force in the short range but attractive force in the medium range while the  $\sigma$ -exchange, the  $\eta$ -exchange and the  $\eta'$ -exchange provide attractive force.

## IV. NUMERICAL RESULTS

The time-independent Schrödinger Equation is

$$\left[ -\frac{\hbar^2}{2\mu} \nabla^2 + V(\vec{r}) - E \right] \Psi(\vec{r}) = 0. \quad (40)$$

However, in our effective potential  $V(\vec{r})$  there exist terms related to  $\nabla^2$ . Thus for the convenience of algebraic manipulation, we separate these momentum-dependent terms from the potential and write the Schrödinger Equation in the form,

$$\left[ -\frac{\hbar^2}{2\mu} \nabla^2 - \frac{\hbar^2}{2\mu} (\nabla^2 \alpha(r) + \alpha(r) \nabla^2) + V_0(\vec{r}) - E \right] \Psi(\vec{r}) = 0, \quad (41)$$

in which  $\alpha(r)$  has form

$$\alpha(r) = (-2\mu) \left( \frac{g_{\sigma\Lambda\Lambda}^2}{4\pi} \frac{1}{2} \mathcal{F}_{4b} - \frac{g_{\Lambda\Lambda\omega}^2}{4\pi} \frac{3}{2} \mathcal{F}_{4b} \right) \quad (42)$$

In our calculation, we take the Laguerre polynomials as a complete set of orthogonal basis to construct the radial wave function. The normalized basis is

$$\chi_{nl}(r) = \sqrt{\frac{(2\lambda)(2l+3)n!}{\Gamma(2l+3+n)}} r^l e^{-\lambda r} L_n^{2l+2}(2\lambda r), \quad n = 1, 2, 3, \dots, \quad (43)$$

which satisfies

$$\int_0^\infty \chi_i(r) \chi_j(r) r^2 dr = \delta_{ij}. \quad (44)$$

Then the total wave function can be written as

$$\Psi(\vec{r}) = \sum_{i=0}^{n-1} a_i \chi_{i0}(r) |\Psi_S\rangle \quad (45)$$

for the S-wave ( $L = 0$ ) of the  $\Lambda\bar{\Lambda}$  system. With this wave function, the spin-orbit interaction operator  $\vec{S} \cdot \vec{L}$  is 0. The spin-spin interaction operator  $\vec{\sigma}_1 \cdot \vec{\sigma}_2$  is 1 for the state  $^3S_1$  and  $-3$  for the state  $^1S_0$ . And, the tensor operator  $\vec{S}_{12}$  is 0 for both states  $^3S_1$  and  $^1S_0$ . Now with the initial state  $|i\rangle$  and the final state  $|f\rangle$  the Hamiltonian of Schrödinger Equation can be written in the following matrix form,

$$\begin{aligned}H_{ij} &= \int_0^\infty a_i \chi_{i0}(r) \left[ -\frac{\hbar^2}{2\mu} (1 + \alpha(r)) \nabla^2 a_j \chi_{j0}(r) \right. \\ &\quad \left. - \frac{\hbar^2}{2\mu} \nabla^2 (\alpha(r) a_j \chi_{j0}(r)) \right. \\ &\quad \left. + V(r, \vec{S} \cdot \vec{L} = 0) a_j \chi_{j0}(r) \right] r^2 dr.\end{aligned}\quad (46)$$

Digitalizing this matrix one can obtain the eigenvalue and the eigenvector. If a negative eigenvalue is obtained, a bound

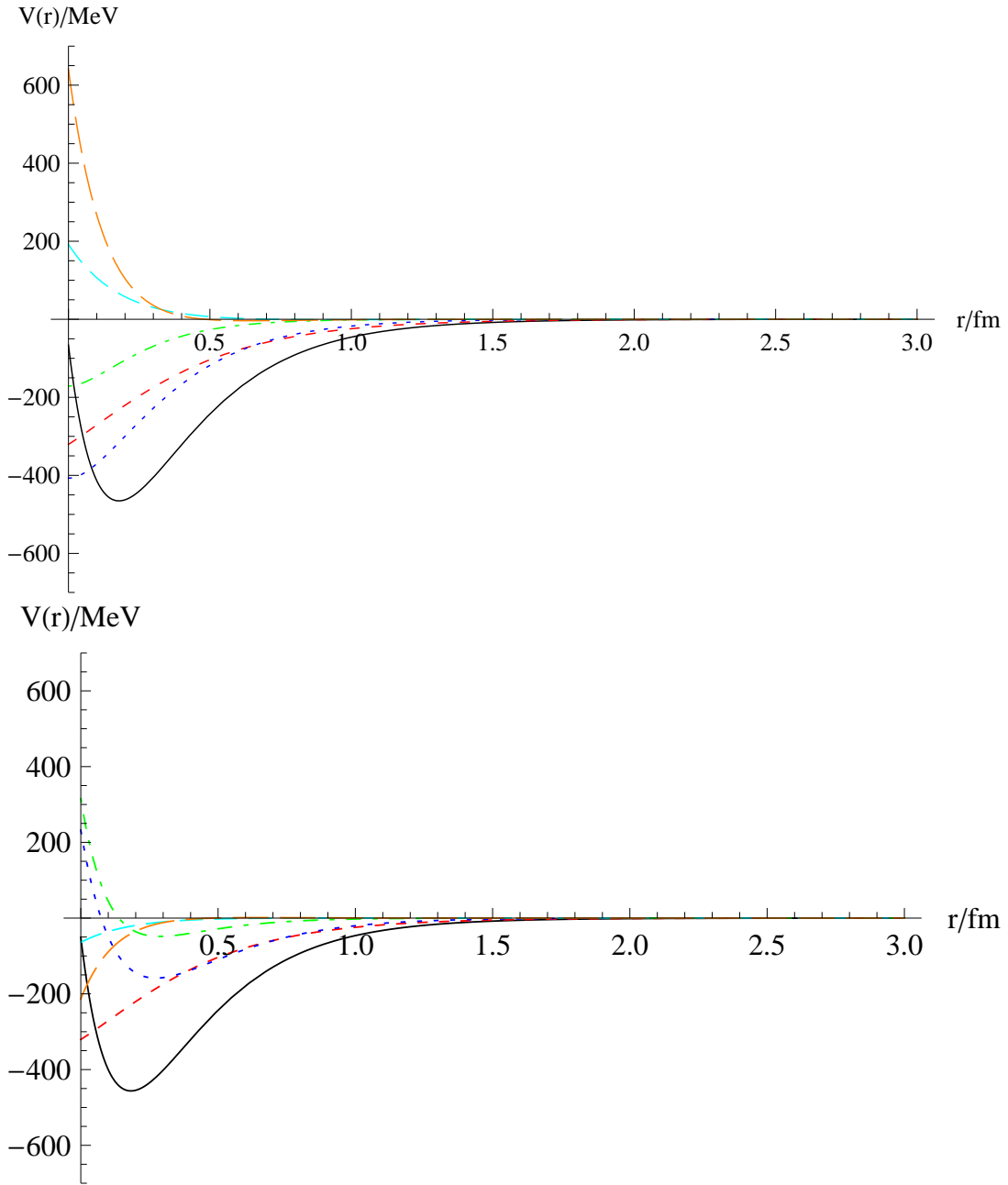


FIG. 3: (Color online) The effective potentials of the system  $\Lambda\bar{\Lambda}$  with the parameters given in Table I. The up one is for the state  $^1S_0$  while the down one is for the state  $^3S_1$ . The solid line represents the total potential. The three dashed lines, short, medium and long, represent the contributions of the  $\sigma$ ,  $\eta$  and  $\eta'$  exchanges respectively. The contributions of the  $\omega$ -exchange is denoted by the dotted line while that of the  $\phi$ -exchange is reflected by the dot-dashed line.

state exists. In our calculation, we apply a computational program which is based on the variational method. We first vary the parameter  $\lambda$  to get the lowest value, then change the trial wave function to reach a stable result.

For the cutoff parameter, we adopt the reasonable range as  $900\text{MeV} \sim 2000\text{MeV}$  and follow the rule that the heavier the mass is, the bigger the cutoff parameter is. Given that both the  $\eta$ -exchange and the  $\eta'$ -exchange provide repulsive

force for the state  $^1S_0$  but attractive force for the state  $^3S_1$ , we fix the cutoff parameter to be  $\Lambda_\eta = 1900\text{ MeV}$  for the  $\eta$ -exchange and  $\Lambda_{\eta'} = 2000\text{ MeV}$  for the  $\eta'$ -exchange to obtain the largest differences between the states  $^1S_0$  and  $^3S_1$ . For the other cutoff parameters for the  $\sigma$ -exchange,  $\omega$ -exchange and  $\phi$ -exchange, we tune them in the range  $900\text{MeV} \sim 2000\text{MeV}$  to obtain the negative and stable eigenvalue  $E$  for the states  $^1S_0$  and  $^3S_1$ . The numerical results are shown in Table II. Our

TABLE II: Binding energies of the states  $\Lambda\bar{\Lambda}(^3S_1)$  and  $\Lambda\bar{\Lambda}(^1S_0)$  with different sets of  $\Lambda_\sigma$ ,  $\Lambda_\omega$  and  $\Lambda_\phi$ . The cutoff parameter for the  $\eta$ -exchange and  $\eta'$ -exchange are fixed to be  $\Lambda_\eta = 1900$  MeV and  $\Lambda_{\eta'} = 2000$  MeV respectively.

$\Lambda_\sigma$ (MeV)	$\Lambda_\omega$ (MeV)	$\Lambda_\phi$ (MeV)	E (MeV)	
			$^3S_1$	$^1S_0$
900	1050	1100	-59.054	-15.316
925	1075	1125	-88.148	-25.218
950	1100	1150	-124.938	-38.011
975	1125	1175	-170.972	-53.989
1000	1150	1200	-228.668	-73.517

results indicate that when the cutoff parameters are adopted as  $\Lambda_\sigma \in (900 \sim 1000$  MeV),  $\Lambda_\omega \in (1050 \sim 1150$  MeV) and  $\Lambda_\phi \in (1100 \sim 1200$  MeV), we obtain loosely bound states of  $\Lambda\bar{\Lambda}(^1S_0)$ , with binding energy being  $-15.316 \sim -73.517$  MeV. The binding of the state  $\Lambda\bar{\Lambda}(^3S_1)$  is much deeper, with binding energy being  $-59.045 \sim -228.668$  MeV, see Table II.

Meanwhile, we also perform an investigation of the dependence of the binding energies on  $\Lambda_\sigma$ ,  $\Lambda_\omega$  and  $\Lambda_\phi$ . During our study, we change one of the above three parameters in its proper range while keeping the other two to be their lowest value. The cutoff parameter for the individual meson should be larger than mass of the exchanged meson, so the lowest values of the cutoff parameters can be taken as  $\Lambda_\sigma = 900$  MeV,  $\Lambda_\omega = 900$  MeV, and  $\Lambda_\phi = 1100$  MeV. We plot the variation of the binding energy with individual cutoff parameter in Fig. 4.

From the curves of Fig 4, we see that the binding energies of both  $^1S_0$  and  $^3S_1$  depend most sensitively on  $\Lambda_\omega$  and least sensitively on  $\Lambda_\phi$ . Since the solutions changes dramatically when the cutoff parameter of the  $\omega$ -exchange increases, it seems that we should to take  $\Lambda_\omega < 1000$  MeV. On the other hand, the binding energy changes very slowly with  $\Lambda_\phi$ , so we fix the cutoff parameter of the  $\phi$ -exchange between 1700 MeV and 1800 MeV. Given the sigma is lighter than the omega, we take  $\Lambda_\sigma = 900$  MeV. Based on these analysis, we tabulated the numerical results in Table III. From Table III, we can see that when the cutoff parameters are taken as  $\Lambda_\sigma = 900$  MeV,  $\Lambda_\omega \in (900 \sim 1000$  MeV) and  $\Lambda_\phi \in (1700 \sim 1800$  MeV), we obtain a loosely bound state of  $\Lambda\bar{\Lambda}(^1S_0)$ , with binding energy around  $-7.624 \sim -13.290$  MeV. The state  $\Lambda\bar{\Lambda}(^3S_1)$  is also a loosely bound state, with slightly larger binding energy around  $-50.389 \sim -82.744$  MeV.

The threshold of  $\Lambda\bar{\Lambda}$  is 2231.3 MeV. If  $Y(2175)$  and  $\eta(2225)$  are regarded as bound states of  $\Lambda\bar{\Lambda}(^3S_1)$  and  $\Lambda\bar{\Lambda}(^1S_0)$ , the binding energies should be  $-56.37$  MeV and  $-6.37$  MeV respectively, both of which roughly lie in the range of the our results,  $-50.4 \sim -82.7$  MeV for state  $\Lambda\bar{\Lambda}(^3S_1)$  and  $-7.6 \sim -13.3$  MeV for states  $\Lambda\bar{\Lambda}(^1S_0)$ . From Table III, we can also tell that the difference between the binding energy of the state  $^3S_1$  and that of the state  $^1S_0$  increases slowly when the attractive forces coming from the  $\omega$ -exchange and  $\phi$ -exchange increase. Besides, we also notice that the difference of the binding energy between these two

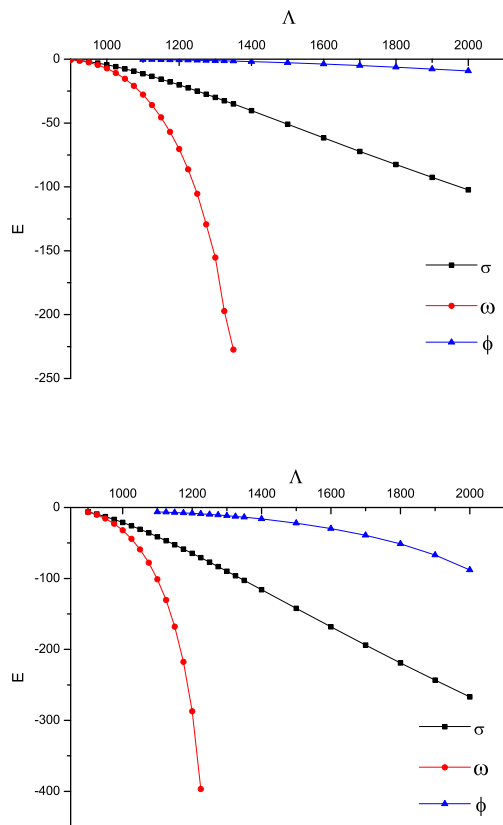


FIG. 4: (Color online) The dependence of the binding energy on  $\Lambda_\sigma$ ,  $\Lambda_\omega$  and  $\Lambda_\phi$  for the states  $^1S_0$  (left) and  $^3S_1$  (right). The cutoff parameters for the  $\eta$ -exchange and  $\eta'$ -exchange are fixed to be  $\Lambda_\eta = 1900$  MeV and  $\Lambda_{\eta'} = 2000$  MeV respectively.

states is  $43 \sim 69$  MeV, which is consistent with the difference between the thresholds of  $Y(2175)$  and that of  $\eta(2225)$ . This prominent feature seems to indicate that  $Y(2175)$  and  $\eta(2225)$  might be regarded as the bound states of  $\Lambda\bar{\Lambda}(^3S_1)$  and  $\Lambda\bar{\Lambda}(^1S_0)$  respectively.

Besides, we also perform a study of the hidden-charm partner of  $\Lambda\bar{\Lambda}$  because of the similarity of the  $\Lambda\bar{\Lambda}$  and  $\Lambda_c\bar{\Lambda}_c$  systems. Actually, in Ref. [20] the authors have studied the baryonium  $\Lambda_c\bar{\Lambda}_c$ . However, they omit the term related to  $\mathcal{F}_4$  (see Eq. 32) which also appears in the study of the deuteron [18]. We first reproduce their results with our program and then focus on the contribution of the terms related to  $\mathcal{F}_4$  in the formation of the bound states of  $\Lambda_c\bar{\Lambda}_c$  and  $\Lambda\bar{\Lambda}$ . We summarize our results in Tables IV, V and VI.

Our result indicates that the terms related to  $\mathcal{F}_4$  have tiny influence on the bound state of the hidden-charm  $\Lambda_c\bar{\Lambda}_c$ , see Table IV. These terms also change the binding of the bound state of  $\Lambda\bar{\Lambda}(^1S_0)$  very little, see Table V. However, these terms can deepen the binding of the state  $\Lambda\bar{\Lambda}(^3S_1)$  significantly when binding energy of the state  $\Lambda\bar{\Lambda}(^3S_1)$  reaches tens of MeV. For example, when the cutoff parameter is fixed to be 1100 MeV,

TABLE III: The binding energies of the states  $\Lambda\bar{\Lambda}(^1S_0)$  and  $\Lambda\bar{\Lambda}(^3S_1)$  with the  $\Lambda_\sigma = 900$  MeV,  $900 \text{ MeV} < \Lambda_\omega < 1000$  MeV and  $1700 \text{ MeV} < \Lambda_\phi < 1800$  MeV. The cutoff parameters for the  $\eta$ -exchange and  $\eta'$ -exchange are fixed to be  $\Lambda_\eta = 1900$  MeV and  $\Lambda_{\eta'} = 2000$  MeV respectively.

			E (MeV)	
$\Lambda_\sigma$ (MeV)	$\Lambda_\omega$ (MeV)	$\Lambda_\phi$ (MeV)	$^3S_1$	$^1S_0$
900	925	1700	-50.389	-7.624
900	925	1750	-57.221	-8.441
900	925	1800	-64.950	-9.290
900	950	1700	-64.891	-11.153
900	950	1750	-73.241	-12.203
900	950	1800	-82.744	-13.290

TABLE IV: The contribution of the term  $\mathcal{F}_4$  in forming the bound state of  $\Lambda_c\bar{\Lambda}_c(^1S_0)$ .  $\Lambda$  is the cutoff parameter. The result without  $\mathcal{F}_4$  (original) comes from Ref. [20].

E (MeV)		
$\Lambda$ (MeV)	original	$\mathcal{F}_4$ added
890	-2.80	-2.88
900	-4.61	-4.75
1000	-49.72	-53.20
1100	-142.19	-160.115

the binding energy of the state  $\Lambda\bar{\Lambda}(^3S_1)$  is  $-57.974$  MeV without the terms  $\mathcal{F}_4$ -related terms. However, it changes into  $-101.066$  with the  $\mathcal{F}_4$ -related terms included, see Table VI.

In Ref. [20], the authors also studied the spin-triplet  $\Lambda_c\bar{\Lambda}_c$  where the S-D mixing effect may be important. In their study, they related the coupling constants of Lambda-Lambda-meson to those of nucleon-nucleon-meson via the quark model. Since there exists  $SU(3)$  - *flavor* symmetry breaking of the coupling constants of nucleon-nucleon-meson, the authors adopted the values  $f_{\omega\Lambda_c\Lambda_c} = -g_{\omega\Lambda_c\Lambda_c}$  which leads to the vanishing S-D mixing. In the present case we take  $f_{\omega\Lambda_c\Lambda_c} = 0$  because  $f_{\omega NN} = 0$ . Now we revisit the spin-triplet  $\Lambda_c\bar{\Lambda}_c$  system. We mainly focus on the effect of the S-D mixing in forming the bound state of  $\Lambda_c\bar{\Lambda}_c$  with spin-triplet. We summarize our results in Table VII. Our result indicates that the effect of the S-D mixing in the formation of the bound state of  $\Lambda_c\bar{\Lambda}_c$  with spin-triplet is quite small. For example, when we set the cutoff parameter to be 900 MeV, the binding energy without the S-D mixing is  $-4.61$  MeV. When we add the S-D mixing, the binding energy is  $-4.40$  MeV with the same cutoff parameter, see Table VII.

TABLE V: The contribution of the terms related to  $\mathcal{F}_4$  in forming the bound state of  $\Lambda\bar{\Lambda}(^1S_0)$ . Here, we adopt the same value for the cutoff parameters of all the exchanged mesons.

E (MeV)		
$\Lambda$ (MeV)	without $\mathcal{F}_4$	with $\mathcal{F}_4$
900	-0.317	-0.274
925	-1.150	-1.140
950	-2.409	-2.492
975	-4.192	-4.474
1000	-6.568	-7.203
1025	-9.580	-10.783
1050	-13.261	-15.316
1075	-17.632	-20.914
1100	-22.711	-27.703

TABLE VI: The contribution of the terms related to  $\mathcal{F}_4$  in forming the bound state of  $\Lambda\bar{\Lambda}(^3S_1)$ . Here, we adopt the same value for the cutoff parameters of all the exchanged mesons.

E (MeV)		
$\Lambda$ (MeV)	without $\mathcal{F}_4$	with $\mathcal{F}_4$
900	-6.549	-6.258
925	-9.728	-10.125
950	-13.822	-15.52
975	-18.868	-22.742
1000	-24.873	-32.126
1025	-31.823	-44.065
1050	-39.687	-59.054
1075	-48.421	-77.748
1100	-57.974	-101.066

## V. SUMMARY AND DISCUSSION

In the present work, we have used the one-boson-exchange potential (OBEP) model, which works very well in describing the deuteron, to study the system of  $\Lambda\bar{\Lambda}$  with quantum numbers  $J^{PC} = 1^{--}$  and  $0^{-+}$ . We have included the contributions of the pseudoscalar  $\eta$  and  $\eta'$  exchanges, the scalar  $\sigma$ -exchange and the vector  $\omega$  and  $\phi$  exchanges. Since the reasonable range of the cutoff parameter in the study of the deuteron is  $800 \sim 1500$  MeV, we take the range as  $900 \sim 2000$  MeV which is wide enough to study the dependence of the binding solutions on the cutoff parameter. We follow the rule that the

TABLE VII: The contribution of the S-D mixing in forming the bound state of  $\Lambda_c \bar{\Lambda}_c$ . Here, we adopt the coupling constant for the  $\omega$ -exchange as  $f_{\omega\Lambda_c\Lambda_c} = 0$ . The results of “original” are taken from Ref. [20].

$\Lambda$ (MeV)	original	E (MeV)	
		$^1S_0$	$^3S_1 - ^3D_1$
890	-2.80	-2.80	-2.66
900	-4.61	-4.61	-4.40
1000	-49.72	-49.72	-46.50
1100	-142.19	-142.19	-130.17

heavier the meson is, the larger the cutoff is and that the cutoff parameter should be larger than the mass of the corresponding exchanged mesons.

Our results indicate that both the  $\eta$ -exchange and the  $\eta'$ -exchange provide repulsive force for the state  $^1S_0$  but attractive force for the state  $^3S_1$ . The  $\sigma$ -exchange provides attractive force for both of these two states. If we fix the cutoff parameters for the  $\eta$ -exchange and the  $\eta'$ -exchange to be  $\Lambda_\eta = 1900$  MeV and  $\Lambda_{\eta'} = 2000$  MeV respectively, we find the binding solutions for both of the two states depend most sensitively on  $\Lambda_\omega$  and least sensitively on  $\Lambda_\phi$ . We also find that the binding of the state  $^1S_0$  is shallower than that of  $^3S_1$  with the same cutoff parameter.

When we fix  $\Lambda_\eta = 1900$  MeV,  $\Lambda_{\eta'} = 2000$  MeV and  $\Lambda_\sigma = 900$  MeV and tune  $\Lambda_\omega$  between 900 MeV and 1000 MeV and  $\Lambda_\phi$  between 1700 and 1800 MeV, we obtain bound states for both  $^1S_0$  and  $^3S_1$ . The binding energies are  $-7.6 \sim -11.3$  MeV and  $-50.4 \sim -82.7$  MeV respectively. Assuming  $Y(2175)$  and  $\eta(2225)$  are bound states of  $\Lambda\bar{\Lambda}(^3S_1)$  and

$\Lambda\bar{\Lambda}(^1S_0)$ , the binding energies should be  $-56.37$  MeV and  $-6.37$  MeV respectively which lie in the ranges of our results,  $-50.4 \sim -82.7$  MeV and  $-7.6 \sim -11.3$  MeV. Most importantly, we also notice that the difference of the binding energies between the state  $^3S_1$  and  $^1S_0$  is  $43 \sim 69$  MeV which is consistent with the difference between the masses of  $Y(2175)$  and  $\eta(2225)$ . Our present calculation suggests that  $Y(2175)$  and  $\eta(2225)$  may be the bound states of  $\Lambda\bar{\Lambda}(^3S_1)$  and  $\Lambda\bar{\Lambda}(^1S_0)$ . The study of their decay patterns within the same framework will be very helpful. In fact, there is some evidence for the  $\Lambda\bar{\Lambda}$  near-threshold enhancement in the  $J/\psi \rightarrow \gamma\Lambda\bar{\Lambda}$  [21], which may be due to the  $\eta(2225)$ .

Because of the similarity of  $\Lambda\bar{\Lambda}$  and  $\Lambda_c\bar{\Lambda}_c$ , we also perform a study of the hidden-charm partner of  $\Lambda\bar{\Lambda}$ . Given that the authors in Ref. [20] have studied the baryonium of  $\Lambda_c\bar{\Lambda}_c$ . We first confirm their results and then focus on the contribution of the terms related to  $\mathcal{F}_4$  in forming the bound states of  $\Lambda\bar{\Lambda}$  and  $\Lambda_c\bar{\Lambda}_c$ . From our results, we find that the contribution of the terms related to  $\mathcal{F}_4$  is small for the system  $\Lambda_c\bar{\Lambda}_c$ . The case of the state  $\Lambda\bar{\Lambda}(^1S_0)$  is similar. However, for the spin-triplet state of  $\Lambda\bar{\Lambda}$ , the  $\mathcal{F}_4$ -related terms change the binding energy significantly when the binding energy is around tens of MeV. We also find the S-D mixing provides quite small contributions in the formation of the spin-triplet state of  $\Lambda_c\bar{\Lambda}_c$ .

## VI. ACKNOWLEDGEMENT

We thank Jian-Ping Dai and Bo-Chao Liu for useful discussions. This work is supported by the National Natural Science Foundation of China under Grant 11035006, 11121092, 11261130311 (CRC110 by DFG and NSFC), the Chinese Academy of Sciences under Project No.KJXC2-EW-N01 and the Ministry of Science and Technology of China (2009CB825200).

- 
- [1] B. Aubert *et al.*, BABAR Collaboration, Phys. Rev. **D74**, 091103 (2006).
  - [2] M. Ablikim *et al.*, BES Collaboration, Phys. Rev. Lett. **100**, 102003 (2008).
  - [3] G.-J. Ding and M.-L. Yan, Phys. Lett. **B650**, 390 (2007).
  - [4] G.-J. Ding and M.-L. Yan, Phys. Lett. **B657**, 49 (2007).
  - [5] Z.-G. Wang, Nucl. Phys. **A791**, 106 (2007).
  - [6] H.-X. Chen, X. Liu, A. Hosaka, and S.-L. Zhu, Phys. Rev. **D78**, 034012 (2008).
  - [7] N. Drenska, R. Faccini, and A. Polosa, Phys. Lett. **B669**, 160 (2008).
  - [8] C. Shen *et al.*, Belle Collaboration, Phys. Rev. **D80**, 031101 (2009).
  - [9] A. Martinez Torres, K. Khemchandani, L. Geng, M. Napsuciale, and E. Oset, Phys. Rev. **D78**, 074031 (2008).
  - [10] S. Gomez-Avila, M. Napsuciale, and E. Oset, Phys. Rev. **D79**, 034018 (2009).
  - [11] S.-L. Zhu, Int. J. Mod. Phys. **E17**, 283 (2008). [hep-ph].
  - [12] L. Alvarez-Ruso, J. Oller, and J. Alarcon, Phys. Rev. **D80**, 054011 (2009).
  - [13] C.-Z. Yuan, BES Collaboration, Nucl. Phys. Proc. Suppl. **181-182**, 348 (2008).
  - [14] Z. Bai *et al.*, MARK-III Collaboration, Phys. Rev. Lett. **65**, 1309 (1990).
  - [15] D.-M. Li and B. Ma, Phys. Rev. **D77**, 094021 (2008).
  - [16] C. Dover and M. Goldhaber, Phys. Rev. **D15**, 1997 (1977).
  - [17] X. Liu, Z.-G. Luo, Y.-R. Liu, and S.-L. Zhu, Eur. Phys. J. **C61**, 411 (2009).
  - [18] R. Machleidt, K. Holinde, and C. Elster, Phys. Rept. **149**, 1 (1987).
  - [19] J. Beringer *et al.*, Particle Data Group, Phys. Rev. **D86**, 010001 (2012).
  - [20] N. Lee, Z.-G. Luo, X.-L. Chen, and S.-L. Zhu, Phys. Rev. **D84**, 014031 (2011).
  - [21] M. Ablikim *et al.*, BESIII Collaboration, Phys. Rev. **D 86**, 032008 (2012); J. P. Dai, Ph.D thesis at IHEP (2012).



